ISSN 0030-400X, Optics and Spectroscopy, 2015, Vol. 118, No. 2, pp. 214–223. © Pleiades Publishing, Ltd., 2015.
Original Russian Text © V.A. Minaeva, B.F. Minaev, G.V. Baryshnikov, N.V. Surovtsev, O.P. Cherkasova, L.I. Tkachenko, N.N. Karaush, E.V. Stromylo, 2015, published in Optika i Spektroskopiya, 2015, Vol. 118, No. 2, pp. 227–236.

CONDENSED-MATTER SPECTROSCOPY

Temperature Effects in Low-Frequency Raman Spectra of Corticosteroid Hormones

V. A. Minaeva[a], B. F. Minaev[a,b], G. V. Baryshnikov[a], N. V. Surovtsev[c], O. P. Cherkasova[d], L. I. Tkachenko[a], N. N. Karaush[a], and E. V. Stromylo[a]

[a] *Cherkassy National University, Cherkassy, 18031 Ukraine*
[b] *Tomsk State University, Tomsk, 634050 Russia*
[c] *Institute of Automation and Electrometry, Siberian Branch, Russian Academy of Sciences, Novosibirsk, 630090 Russia*
[d] *Institute of Laser Physics, Siberian Branch, Russian Academy of Sciences, Novosibirsk, 630128 Russia*
e-mail: bfmin@rambler.ru

Received May 16, 2014

Abstract—Experimental Raman spectra of the corticosteroid hormones corticosterone and desoxycorticosterone are recorded at different temperatures (in the range of 30–310 K) in the region of low-frequency (15–120 cm^{-1}) vibrations using a solid-state laser at 532.1 nm. The intramolecular vibrations of both hormones are interpreted on the basis of Raman spectra calculated by the B3LYP/6-31G(d) density functional theory method. The intermolecular bonds in tetramers of hormones are studied with the help of the topological theory of Bader using data of X-ray structural analysis for crystalline samples of hormones. The total energy of intermolecular interactions in the tetramer of desoxycorticosterone (−49.1 kJ/mol) is higher than in the tetramer of corticosterone (−36.9 kJ/mol). A strong intramolecular hydrogen bond $O^{21}-H\cdots O=C^{20}$ with an energy of −42.4 kJ/mol was revealed in the corticosterone molecule, which is absent in the desoxycorticosterone molecule. This fact makes the Raman spectra of both hormones somewhat different. It is shown that the low-frequency lines in the Raman spectra are associated with skeletal vibrations of molecules and bending vibrations of the substituent at the C^{17} atom. The calculated Raman spectrum of the desoxycorticosterone dimer allows one to explain the splitting and shift of some lines and to interpret new strong lines observed in the spectra at low temperatures, which are caused by the intermolecular interaction and mixing of normal vibrations in a crystal cell. On the whole the calculated frequencies are in a good agreement with the experimental results.

DOI: 10.1134/S0030400X15020149

INTRODUCTION

The study of dynamical response of biomolecules in a wide temperature range (from cryogenic to room temperatures) allows one to determine the intra- and intermolecular force constants and potentials by solving the inverse spectral problem and, finally, to predict conformations of biological associates and polymers and their changes with variation of ambient conditions [1–8]. This is especially important for hormones, because it allows their interaction with receptors to be predicted, which is the key problem of biochemistry and biomedicine. Therefore, it is not surprising that the study of temperature dependence of the spectral properties of hormones has received considerable attention [1, 2, 7, 8].

Experiments on neutron scattering for the steroid hormones testosterone and progesterone and their derivatives at 20 and 290 K [1, 2] allowed the assignment of low-frequency vibrations by comparing them to the results of quantum-chemical calculations of IR spectra. Inelastic neutron scattering offers certain advantages over IR spectroscopy in the studies of low-frequency vibrations of molecules and phonons in crystals due to the extension of the range and the change of selection rules [2].

Detailed analysis of the nature of low-frequency vibrations of progesterone, 17α-hydroxyprogesterone, and cortisone was presented in [9]. In this paper, the authors attempted to relate the change in the position of observed absorption bands with variation of temperature from 300 to 18 K to the presence of intermolecular hydrogen bonds.

Earlier, we studied the absorption and Raman spectra of a number of corticosteroid hormones belonging to progestins and glucocorticoids [7–12]. The temperature dependence of Raman lines and terahertz absorption was investigated [7, 8], the quantum-chemical modeling of hormones was performed

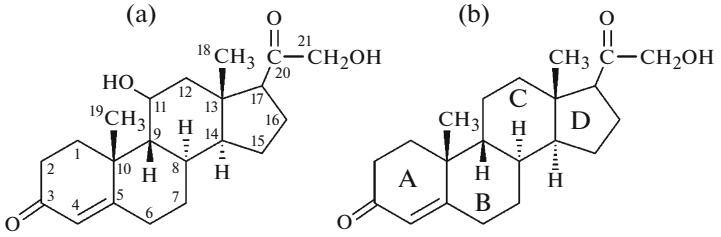

Fig. 1. Structure of molecules (a) CS and (b) DCS. The standard numbering of carbon atoms is shown in (a), and the notation of rings is shown in (b).

at the density functional theory (DFT) level, the observed spectral features were assigned to vibrational modes in molecules [10, 11], and the intra- and intermolecular interactions in crystalline samples of hormones were analyzed [8, 12].

In the present paper, the temperature dependence of low-frequency Raman spectra of the corticosteroid hormones corticosterone (CS) and desoxycorticosterone (DCS) (Fig. 1) was studied. In the human body, these hormones affect water–salt exchange, and, in addition, they exhibit a glucocorticoid activity [13]. CS is formed in mitochondria of cells of adrenal cortex from DCS under the action of the enzyme P450c11 (11β-hydroxylation). The molecules of these hormones are characterized by the presence of a hydroxyl group at the carbon atom C^{11} of the steroid core (Fig. 1). Analysis of the molecular structure of the hormones in question and the character of intermolecular interaction in crystalline samples allowed us to explain the specific features of the temperature dependence of Raman spectra.

EXPERIMENT AND THEORETICAL CALCULATIONS

Synthetic steroid hormones CS (4-pregnen-11β, 21-diol-3, 20-dione) and DCS (4-pregnen-21-ol-3, 20-dione) from the Koch-Light Laboratories Ltd were used without additional purification.

Fine crystalline powders of hormones were pressed into tablets 8 mm in diameter. The Raman spectra were recorded with a TriVista 777 triple grating spectrometer using a line of 532.1 nm of a solid-state Millenia Pro laser. The light power focused to a strip 50 μm in width and 250 μm in length was about 70 mW. The experiment on recording Raman scattering from the samples was conducted with the nominal scattering geometry at the angle of 90° without polarization selection. The spectra were measured in the temperature range of 30–310 K, and the photoluminescence contribution was subtracted in the form of a cubic polynomial and, in some cases, by using a linear approximation. The Raman spectra were recorded using the facilities of the High-Resolution Spectroscopy of Gases and Condensed Matter Center for Collective Use of the Institute of Automation and Electrometry of the Siberian Branch of the Russian Academy of Sciences.

Normal vibrations (NVs) and vibrational spectra of molecules of the hormones under study were calculated by the DFT method [14, 15] with the B3LYP functional and the 6-31G(d) basis set using the Gaussian 03 program package [16]. The applicability of this calculation method to prediction of the frequencies, forms of vibrations, and intensities of lines in the Raman spectra of steroid hormones was demonstrated in [7, 17]. All the NV frequencies are real, which indicates that the true minimum on the total energy hypersurface of molecules was found. The calculated NV frequencies were compared to the experimental frequencies without using a scaling factor.

Molecular crystals of the hormones studied belong to the $P2_1$ monoclinic space group. Parameters of elementary cells are listed in Table 1.

Structural information on the hormones in question (Table 1) is somewhat controversial. For example, it was reported in earlier papers published in 1973 that the elementary cells of CS [18, 20] and DCS [20, 21] contain two molecules. However, it followed from the results of [22] that the elementary cell of DCS contained four molecules. The data available in the literature on nonvalence interactions in the crystal structures of CS and DCS are incomplete. The authors of [18, 20] pointed to the existence of intermolecular hydrogen bonds in the cell of CS between the oxygen atom of a ketone group at C^3 of ring A and the hydrogen atom of a hydroxyl group at C^{11} of a neighboring molecule. According to [20, 21], there are no intermolecular hydrogen bonds in a DCS crystal and the molecules are bound by the van der Waals forces. R. Dey et al. [22] reported evidence for the presence of intramolecular hydrogen bonds $O^{20}\cdots H^{16}$, $O^{20}\cdots H^{18}$, $O^{20}\cdots H^{21}$ in DCS (Fig. 1).

To study the nonvalence interactions in the crystal structures of CS and DCS, we chose fragments of crystals consisting of two elementary crystal cells with the experimental geometric parameters *a*, *b*, and *c* reported in [19, 21]. In our opinion, such model

Table 1. Description of data on the structures of the substances studied

Substance		Corticosterone	Desoxycorticosterone
Molecular formula		$C_{21}H_{30}O_4$	$C_{21}H_{30}O_3$
Molecular mass, g/mol		346.5	330.4
Crystal system		monoclinic	Monoclinic
Symmetry group		$P2_1$ [18, 19]	$P2_1$ [21, 22]
Number of molecules in a cell		2 [18–20]	2 [20, 21] 4 [22]
Parameters of the elementary cell *a*, *b*, *c* (Å)	α	90° [18, 19]	90° [21, 22]
	β	97.25° [18] 90° [19]	98.01° [21] 100. 94° [22]
	γ	90° [18, 19]	90° [21, 22]
	a	8.992 [18] 8.308 [19]	8.718 [21] 11.706 [22]
	b	12.293 [18] 12.192 [19]	12.509 [21] 11.171 [22]
	c	8.322 [18] 8.953 [19]	8.481 [21] 13.966 [22]
Volume of the cell (Å^3)		912.5 [18] 906.86 [19]	915.8 [21] 1793.11 [22]
Intramolecular hydrogen bonds			$O^{20}\cdots H^{16}$, $O^{20}\cdots H^{18}$, $O^{20}\cdots H^{21}$ [22]
Intermolecular hydrogen bonds		$C^3{=}O\cdots HO(C^{11})$ [18, 20]	

objects provide more reliable results than the elementary crystal cell containing two molecules.

In the calculation of intermolecular interactions in the hormones crystals, we used an additive scheme of decomposition of a crystal package of four hormone molecules into six dimer pairs. For the selected dimers, we performed the DFT calculation of the Kohn–Sham orbitals with the B3LYP functional in the 6-31G(d) basis set [14, 23]. With the results obtained, the electron density function ρ(**r**) was analyzed in terms of the Bader theory the Quantum Theory of Atoms in Molecules (QTAIM) [24]. This method rigorously defines the criterion for the existence of a chemical bond (the bonding interatomic interaction): the presence of a bond critical point (CP) and a bond path between interacting atoms is, according to this theory, the necessary and sufficient condition for the existence of a chemical bond. The QTAIM method allows one to reveal even very weak interatomic interactions in crystals and isolated molecules (of the H···H, CH···O type, etc.), which are very difficult to detect experimentally.

The energy of intermolecular bonds in dimers and the energy of intramolecular nonvalence interactions were determined using the correlation formula proposed by Espinosa [25, 26]

$$E = 0.5v(\mathbf{r}),$$

where $v(\mathbf{r})$ is the potential energy density (in au) at the corresponding critical point of the bond.

RESULTS AND THEIR DISCUSSION

The CS hormone molecule differs from the DCS molecule by the presence of a hydroxyl group at the C^{11} carbon atom. The presence of the $O^{11}H$ group has a specific effect on the electron density in the B and C rings of the CS molecule (Fig. 1). In particular, the hydroxyl group strongly polarizes the C^{11} atom ($q = +0.13e$), which induces a weak polarization of adjacent C^9 and C^{12} atoms via the σ-core. If the $O_{11}H$ group is absent (in the DCS molecule), the C^{11} atom acquires a characteristic negative charge ($q = -0.29e$) caused by polarization of the CH bonds. The appearance of an additional hydroxyl group leads to an increase in the dipole moment from 2.00 D in DCS to 2.13 D in CS. The absence of the $O^{11}H$ group in the DCS molecule does not change significantly the bond lengths and valence angles as compared to the CS molecule but considerably modifies the dihedral angles. The changes are most considerable (from 6° to 9°) for

Table 2. Frequencies, activities, and forms of intermolecular vibrations in the spectrum of the DCS dimer calculated by the DFT method in the B3LYP 6-31G(d) approximation

Vibration	NV	ν, cm^{-1}	S_i
Out-of-phase translational vibration along the *a* axis	ν_1	6	0.06
Out-of-phase translational vibration along the *c* axis	ν_2	11	0.32
Out-of-phase translational vibration along the *c* axis	ν_3	14	0.34
Out-of-phase librational vibration	ν_4	22	0.37
In-phase librational vibration	ν_5	28	0.63

Note. NV is a normal vibration, S_i is the activity of NV, $Å^4$/amu.

the dihedral angles $C^{11}C^9C^{10}C^5$, $C^{11}C^9C^{10}C^1$, and $C^{11}C^9C^{10}C^{19}$, which characterize the conformation of ring A, and the angles $C^8C^9C^{11}C^{12}$ and $C^9C^{11}C^{12}C^{13}$ in ring C (4°). It is known that the dihedral angles are responsible for occurrence of a very specific conformation of hormones, which, in turn, governs their characteristic biological properties (in view of the spatial specificity of a hormone interaction with a receptor in a living cell) and also their physico-chemical properties [27, 28]. It is assumed that the mineralocorticoid properties of hormones are associated with the rigidity of ring C and the glucocorticoid properties—with the rigidity of ring A [13, 29]. The CS molecule conformation provides a more efficient bonding of this molecule with the glucocorticoid receptor [29], which significantly changes its biological activity as compared to DCS [13].

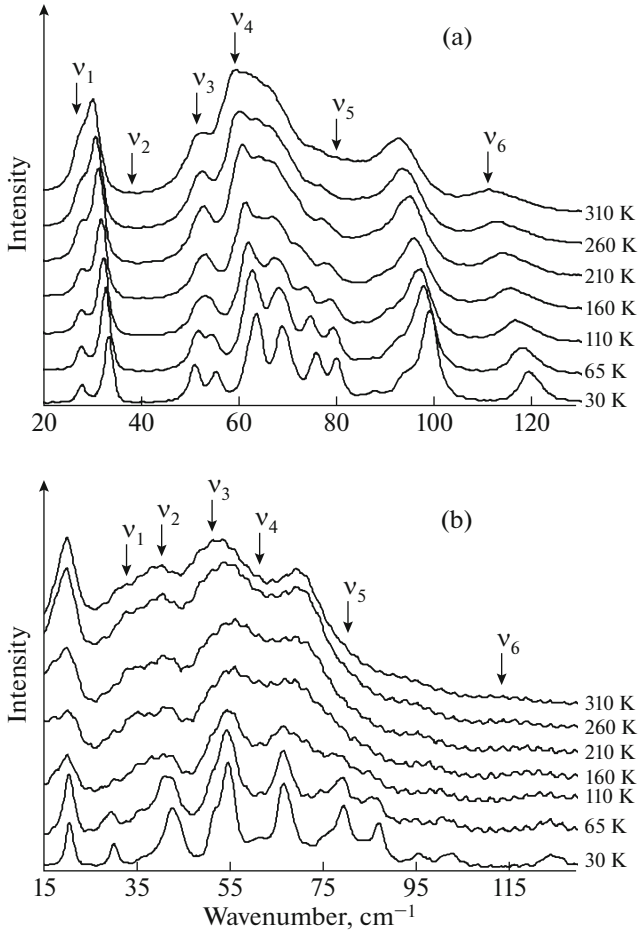

Fig. 2. Raman spectra of (a) CS and (b) DCS at different temperatures. The assignment of frequencies ν_1–ν_6 corresponds to the theoretically calculated normal vibrations.

We assume that the conformation and rigidity of the skeleton, in conjunction with specific features of intermolecular interactions in crystal samples of the hormones studied, have a significant effect on the energy of low-frequency vibrations, which is actually observed at close inspection of the Raman spectra and their temperature dependence.

The experimental Raman spectra of the hormones under study in the frequency region 15–130 cm^{-1} are shown in Fig. 2. For convenience, the spectra are shifted along the ordinate axis. The calculated frequencies, activities, and forms of NVs in the Raman spectra of the isolated CS and DCS molecules and the dimer of DCS are summarized in Table 3. The intermolecular vibrations ν_1–ν_5 calculated for the DCS dimer are presented in a separate table (Table 2).

The Raman spectra of the studied hormones recorded in the region of 15–130 cm^{-1} have several intense lines (Fig. 2). As the temperature is lowered down to 30 K, the line widths decrease, the spectral resolution becomes better, the lines are shifted toward higher frequencies (Fig. 3), and new Raman lines appear. The temperature dependence of intensity of the Raman lines has a complicated character and includes the temperature dependence of the Bose–Einstein factor.

The first three lines in the Raman spectra of CS (at 30, 53, and 59 cm^{-1}) and DCS (at 19, 41, and 54 cm^{-1}) are shifted by 3–4.5 cm^{-1} upon lowering the temperature down to 30 K (Fig. 3a). New lines that will be explained by the DFT calculation of vibrations of an associate composed of two molecules also appear in this case. Here, we will restrict ourselves to an analysis

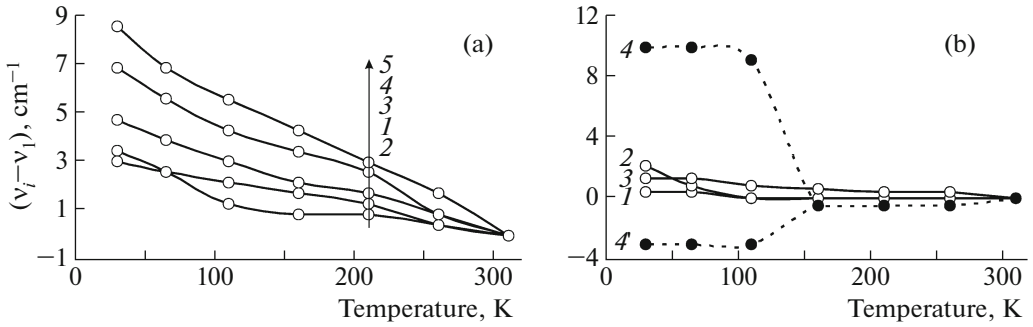

Fig. 3. Temperature dependences of frequency shifts of the Raman lines of (a) CS and (b) DCS. The lines of CS: (*1*) 30, (*2*) 53, (*3*) 59, (*4*) 93, and (*5*) 112 cm^{-1}. The lines of DCS: (*1*) 19, (*2*) 41, (*3*) 54, and (*4* (*4'*)) 70 cm^{-1}.

of NVs calculated for the isolated CS and DCS molecules. According to the quantum-chemical calculations, the experimental line in the spectrum of CS at 30 cm^{-1} (Fig. 2a) belongs to swinging of the skeleton of the molecule with folding and unfolding, which is called by spectroscopists the butterfly vibration (Table 3, the ν_1 normal vibration with a calculated frequency of 28 cm^{-1}). Swinging of the skeleton without bending (the ν_2 normal vibration at a frequency of 39 cm^{-1}) does not manifest itself as a separate line in the Raman spectrum of hormone CS because of a low intensity.

The ν_1 normal vibration with a calculated frequency of 32 cm^{-1} corresponds in the experimental Raman spectrum of hormone DCS to the weak shoulder in the left wing of the band at 41 cm^{-1}. This shoulder forms a separate line on lowering the temperature down to 65 K (Fig. 2b). In our opinion, the first exper-

Table 3. Frequencies, activities, and forms of the NVs in the Raman spectra of CS and DCS calculated by the DFT method in the B3LYP 6-31G(d) approximation. (The experimental frequencies are shown in bold.)

Vibration	CS			DCS			DCS dimer		
	NV	ν, cm^{-1}	S_i	NV	ν, cm^{-1}	S_i	NV	ν, cm^{-1}	S_i
Swinging of the whole skeleton with folding and unfolding	ν_1	28 **(30)**	1.03	ν_1	32 **(30)**	1.18	ν_6	30	0.33
							ν_7	37	0.77
Swinging of the skeleton without bending	ν_2	39	0.21	ν_2	39 **(41)**	0.42	ν_8	41	1.17
							ν_9	47	0.79
Swinging of the skeleton (mainly, rings A and D) and the fragment at C^{17}	ν_3	52 **(53)**	0.79	ν_3	51 **(54)**	0.43	ν_{11}	60	1.80
Swinging of the skeleton (mainly, ring A) and the fragment at C^{17}	ν_4	60 **(59)**	0.60	ν_4	59 **(54)**	0.40	ν_{10}	55	0.89
							ν_{12}	62	0.15
Swinging of the skeleton, twisting of the fragment at C^{17}	ν_5	79 **(93)**	1.33	ν_5	80 **(70)**	1.31	ν_{13}	69	1.19
							ν_{14}	70	0.74
							ν_{15}	77	1.47
							ν_{16}	90	0.30
Twisting of the fragment at C^{17}, r(C^{21}H$_2$)	ν_6	112 **(112)**	0.25	ν_6	113	0.32	ν_{17}	104	0.04
							ν_{18}	108	0.23
Swinging of the skeleton, r(C^{21}H$_2$)	ν_7	125	0.63	ν_7	126	0.59	ν_{19}	121	0.62
							ν_{20}	129	0.64

NV is a normal vibration, S_i is the activity of NV, Å^4/amu; r is the rocking vibration, τ is the twisting vibration.

imental line (at 19 cm^{-1}) is associated with intermolecular vibrations. The ν_2 normal mode in the spectrum of DCS has a higher calculated intensity (S_2 = 0.42 Å^4/amu) than in the spectrum of CS (S_2 = 0.21 Å^4/amu); therefore, it forms a separate line in the experimental spectrum at 41 cm^{-1} (the calculated value is 39 cm^{-1}). This line becomes more distinct with decreasing temperature (Fig. 2b).

The lines at 53 and 59 cm^{-1} in the Raman spectrum of hormone CS (normal vibrations ν_3 and ν_4) correspond to a swinging of the whole skeleton of the molecule with more pronounced torsional vibrations of rings A and D and the fragment at C^{17} (Table 3). The ν_3 and ν_4 normal vibrations, the frequencies and intensities of which are close to each other (the calculated values are 51 and 59 cm^{-1} and 0.43 and 0.40 Å^4/amu, respectively), form one experimental line at 54 cm^{-1} in the spectrum of DCS (Fig. 2b).

It should be noted that the structure of vibrational lines becomes more complicated on lowering the temperature for all the hormones studied (Fig. 2), which can be associated with the imposition of hindered rotation of molecules about crystal axes and other changes in mutual positions of particles on the intramolecular vibrational motion. Polarizability of molecules changes under the action of crystal surroundings, which governs the intensity of Raman lines.

The large frequency shift (7–9 cm^{-1}) on lowering the temperature (Fig. 3a) is observed for lines at 93 and 112 cm^{-1} in the Raman spectrum of hormone CS associated with twisting vibrations of the fragment at C^{17} (the ν_5 and ν_6 normal vibrations with the calculated frequency values 79 and 112 cm^{-1}, respectively). In the experimental spectrum of DCS the line corresponding to the ν_6 normal mode is too weak to be observed at temperatures higher than 65 K, although the frequencies and intensities calculated for the ν_6 normal mode of isolated molecules of CS and DCS have close values (112 and 113 cm^{-1} and 0.25 and 0.32 Å^4/amu, respectively). At lower temperatures, the ν_6 line intensity in the Raman spectrum of DCS is sufficiently high for the line to be observed (Fig. 2b).

In comparing the spectra of CS and DCS, it is necessary to emphasize the shift of the experimental line at 93 cm^{-1} relative to the theoretical value of 79 cm^{-1} calculated for the ν_5 normal mode of an isolated CS molecule and the shift of the analogous line by 10 cm^{-1} toward lower frequencies in the spectrum of DCS (Table 3, Fig. 2). The temperature shift of this line in the experimental spectrum of CS is 9 cm^{-1} on cooling to 30 K (the upper curve in Fig. 3a). At the same temperature (30 K), the ν_5 line in the spectrum of DCS is split into three components (Fig. 2b). The illegible form of this line in the DCS spectrum at different temperatures does not allow us to quantitatively estimate the temperature shift; however, the final splitting, starting with 110–90 K is sufficiently distinct. In Fig. 3b this splitting is shown by curves *4* and *4'*. One can see in Fig. 3b that the curves *4* and *4'* exhibit different temperature shifts of components of the ν_5 band. Curve *4''* is not shown in Fig. 3b because of a too large temperature shift (18 cm^{-1}).

Because the CS and DCS are isostructural (Table 1), the above distinctions can be accounted for by differences in the intermolecular interactions in the crystal forms of the hormones in question. The low-frequency molecular vibrations are very sensitive to such interactions [9].

The calculation of intermolecular interactions by the Bader method in the crystal package consisting of four CS molecules revealed 18 intermolecular bonds stabilizing the tetramer with the total energy −36.9 kJ/mol. Of these bonds, two very weak hydrogen bonds are formed by the ketone group $C^3{=}O$, $C^3{=}O\cdots H(C^{21})$ and $C^3{=}O\cdots H(C^{17})$, which are present in dimer 1–4, with energies of −3.9 and −2.2 kJ/mol and bond lengths 2.712 and 2.964 Å, respectively (Fig. 4a) and 15 nonvalence bonds H···H with the total energy −28.6 kJ/mol and one bond $C^3\cdots H(C^{12})$ in dimer 1–4 with the energy of −2.1 kJ/mol. Of the hydrogen–hydrogen bonds, the bonds $(C^2)H\cdots H(C^7)$ in dimers 1–2 and 4–3 (Fig. 4a) have the highest energy −3.7 kJ/mol. The DFT calculation does not show that the hydroxyl group $O^{11}H$ is involved in the formation of intermolecular hydrogen bonds with the oxygen atom O^3 (Fig. 1a); however, the hydrogen atom of the $O^{11}H$ group forms several intermolecular H···H bonds: with the atom $H(C^{15})$ in dimers 1–2 and 4–3 with an energy of −1.9 kJ/mol and with the atom $H(C^{19})$ in dimer 4–1 with the energy −1.5 kJ/mol.

We have shown that the hydrogen atom of the hydroxyl group $O^{11}H$ forms a strong intramolecular H···H bond with the hydrogen atom of the methyl group $C^{19}H_3$, the energy of which equals −28.0 kJ/mol and the bond length is 1.734 Å, and the hydrogen atom of the hydroxyl group $O^{21}H$ forms a strong intramolecular hydrogen bond $O^{21}-H\cdots O{=}C^{20}$ with the energy −42.4 kJ/mol and bond length 1.888 Å. It may be for this reason the hydroxyl group $O^{21}H$ does not take part in the formation of intermolecular hydrogen bonds in CS.

The total energy of intramolecular nonvalence interactions in the CS molecule amounts to −70.0 kJ/mol, while it is more than a factor of 4 lower in DCS (−17.0 kJ/mol). In the DCS molecule, in which, in contrast to CS, the hydroxyl group OH at the C^{11} carbon atom is absent, the intramolecular H···H interaction of the hydrogen atom at C^{11} with the hydrogen atom of the methyl group $C^{19}H_3$ (Fig. 1b) also exists, but, unlike the $O^{11}H\cdots H(C^{19}H_3)$ interaction in CS, it is approximately a factor of 3 weaker (E = −7.9 kJ/mol). There exists also an intramolecular $(C^{12})H\cdots H(C^{21})$ interaction with the energy −9.1 kJ/mol, which is

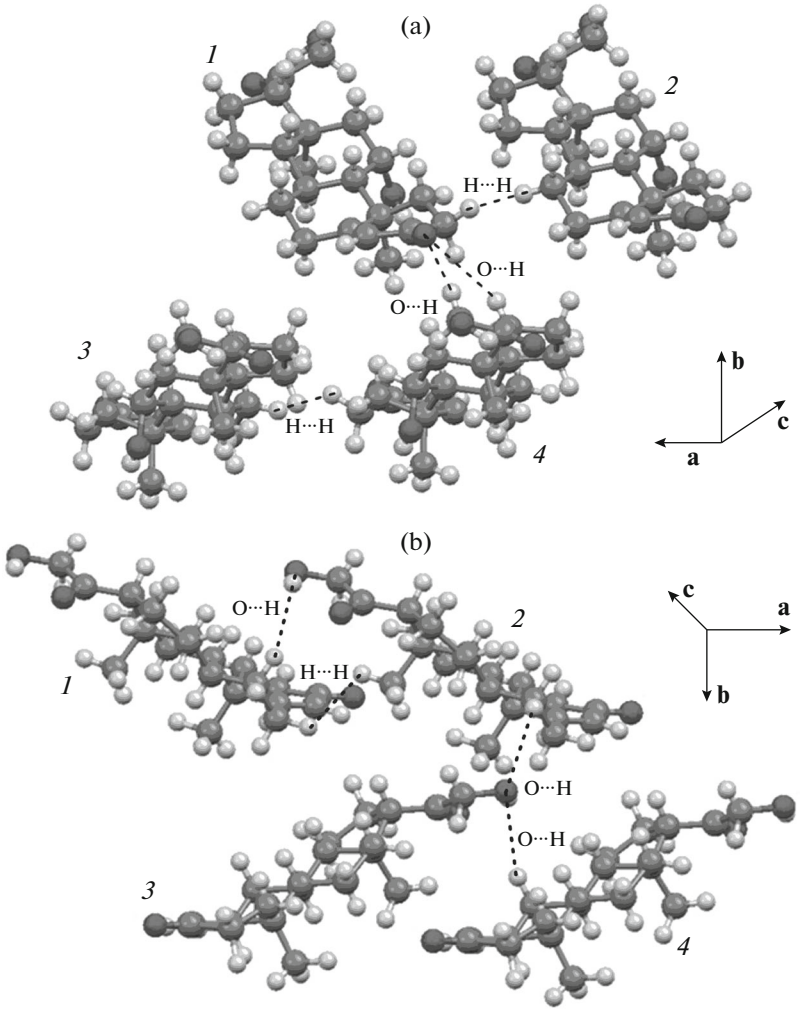

Fig. 4. Some intermolecular interactions in the tetramers of hormones (a) CS, (b) DCS obtained from the analysis of the electron density function by the QTAIM method. (The structures are taken from the PCA data [19, 20].)

much stronger than in CS (–3.5 kJ/mol). The DFT calculations by the Bader method did not reveal the presence of an intramolecular hydrogen bond in the DCS molecule.

The intermolecular interactions in the tetramer of DCS (Fig. 4b) are stronger than in CS ($E = -49.1$ kJ/mol) due to the formation of a larger number of hydrogen bonds. In the DCS tetramer we found ten weak O···H interactions with the total energy –22.3 kJ/mol (for comparison, this energy in CS is –6.1 kJ/mol). The oxygen atom of the hydroxyl group $O^{21}H$ forms hydrogen bonds $(C^7)H\cdots O^{21}-H$ with the energy –4.3 kJ/mol in dimers 1–2 and 4–3 and with the energy –3.7 kJ/mol in dimer 2–3 (Fig. 4b). The O^{21} oxygen atom forms weaker intermolecular hydrogen bonds with the hydrogen atom at C^{14} in dimers 2–1 and 3–4 (the interaction energies are –1.49 and –1.50 kJ/mol).

The differences in the structural parameters of two molecules in the DCS dimer and the distinctions between their intramolecular nonvalence interactions in DCS were revealed by the X-ray structural analysis [22], although our calculations do not confirm the presence of intramolecular hydrogen bonds in crystals of DCS noted in [22].

In contrast to CS, the intermolecular interactions involving the oxygen atom of the ketone group $C^3{=}O$ are very weak in DCS. For example, the $C^3{=}O\cdots H(C^{11})$ interaction calculated for DCS dimers 1–2 and 4–3 has a negligible energy –0.8 kJ/mol. The weak interactions $C^{20}{=}O\cdots H(C^{19}H_3)$, $C^{20}{=}O\cdots H(C^6)$, and $C^{20}{=}O\cdots H(C^9)$ with energies –2.2, –1.6, and –1.5 kJ/mol were predicted by our calculations for dimer 2–3.

Of the intermolecular nonvalence H···H interactions in DCS, the following interactions have the highest energy: $H(C^6)\cdots H(C^{18}H_3)$ in dimers 1–2 (Fig. 4b) and 4–3 with the energy –3.5 kJ/mol and $H(C^6)\cdots H(C^{16})$ in dimers 1–3 and 2–4 with the energy –3.4 kJ/mol.

We found 12 H···H interactions in the DCS tetramer with the total energy −26.8 kJ/mol.

Thus, the capacity of the CS and DCS molecules for intermolecular and intramolecular nonvalence interaction is different, which, in our opinion, leads to distinctions in the experimental Raman spectra of these hormones and their temperature dependences. We explain the significant differences in the position and temperature shift of the ν_5 line in the spectra of CS and DCS relative to the calculated frequency values by the fact that different functional groups take part in the formation of hydrogen bonds. For example, the ketone group $C^3{=}O$ takes part in the formation of intermolecular hydrogen bonds in CS, while in DCS this role is played by the hydroxyl and carbonyl groups of the fragment at C^{17}, the twisting vibrations of which, according to our calculations, are responsible for the appearance of the ν_5 line in the Raman spectrum. Twisting of polar groups $-COCH_2OH$ in the crystal strongly changes molecular polarizability due to intermolecular forces. This fact explains the growth of the ν_5 line intensity under cryogenic conditions because, in this case, the lowest vibrational quanta manifest themselves. For these quanta, the Franck–Condon factors and the electronic structure of molecules in a cell are closely related to the optimized equilibrium structure.

For the lowest quantum number $v = 0$, vibrations of nuclei around the equilibrium position are not affected by anharmonicity, and their wave functions are maximal at this point. Heating of a crystal from 30 to 300 K changes not only the Bose–Einstein distribution, which describes the Raman intensity for the vibrational spectrum, but also the anharmonicity contribution, the Franck–Condon factors, and vibronic mixing of electronic states for vibrational modes of different natures. The last contribution is especially important for the low-frequency modes ($\hbar\omega < k_BT$) that are mixed with crystal phonons and intermolecular vibrations of O···H and H···H bonds. Our analysis of such bonds by the Bader method allows us to understand the qualitative distinction between the temperature dynamics of Raman spectra of CS and DCS crystals (Figs. 2a, 2b, 3a, and 3b).

We more thoroughly interpreted the low-temperature Raman spectrum of DCS on the basis of a DFT calculation of an associate of two molecules (dimer 1–2, Fig. 4b). The geometry of the dimer was optimized starting from the experimental structure (Fig. 4b); some intermolecular distances were constrained to improve the convergence procedure in the optimization process. The calculated Raman spectrum of this dimer of DCS is shown in Fig. 5 and demonstrates good agreement with the low-temperature experimental spectra (Fig. 2b) judging from the number of observed bands and the characters of their shifts. The correlation between normal vibrations ν_6–ν_{20} calculated for the DCS dimer and normal vibrations ν_1–ν_7 calculated for the isolated DCS molecule is shown in Table 3. The splitting of monomolecular modes is associated with the appearance of new degrees of freedom in the dimer. Intermolecular normal vibrations ν_1–ν_5 calculated for the DCS dimer are presented in a separate table (Table 2).

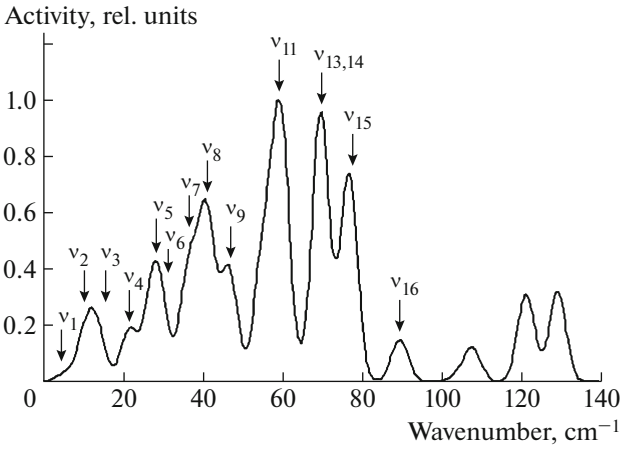

Fig. 5. Raman spectrum calculated by the DFT method for the optimized dimer of DCS. (Raman activity values S_i are normalized to unity.)

On the basis of the calculation of the DCS dimer, the lines at 19 and 30 cm^{-1} in the experimental Raman spectrum (Fig. 2b) are assigned most reliably. The line at 19 cm^{-1} belongs to intermolecular translational vibrations (superposition of three NVs ν_1, ν_2, and ν_3, Table 2, Fig. 5). The ν_1 vibration of the "butterfly" type of the DCS molecule, indicated above for the dimer, is split into two NVs ν_6 and ν_7 with the calculated frequencies of 30 and 37 cm^{-1} (Table 3). The first of these NVs (ν_6 in Fig. 5) corresponds to the line at 30 cm^{-1} in the experimental spectrum in Fig. 2b; however, the main contribution to the intensity of this line is made by the librational vibration (hindered rotation of molecules about the *c* crystal axis) with a calculated frequency value of 28 cm^{-1} (ν_5 in Fig. 5, Table 2). The ν_7 normal vibration, calculated for the dimer, forms a weakly pronounced shoulder in the left wing of the 41-cm^{-1} band, which can be observed in the experimental spectrum of DCS at low temperatures (Fig. 2b).

The translational vibrations (ν_1–ν_3 in Fig. 5, Table 2) manifest themselves in a DCS crystal and yield the first line in the Raman spectrum at 19 cm^{-1} (Fig. 2b). The important result of this calculation is qualitative prediction of nonzero activity of these vibrations in the Raman spectrum. Of interest is also the splitting of the line in the DCS spectrum associated with twisting of the fragment at C^{17} into three new lines (Table 3, ν_5, Fig. 2b; ν_{13}, ν_{14}, ν_{15}, ν_{16} in the dimer, Fig. 5). This occurs because, in the force field of the dimer, the twisting of the fragment at C^{17} generates new types of interactions and

force constants, which hinder the motion of this type. Because the fragment is polar, the Raman scattering of light from such vibrations becomes more intense due to the strong change of polarizability of the dimer. In the dimer model the crystal surroundings is taken into account only partially; clearly, the change of polarizability of a real crystal cell on twisting vibrations of the group $-COCH_2OH$ should be stronger and their intensity in the Raman spectrum will also increase in a more real model of a crystal.

CONCLUSIONS

The experimental Raman spectra of corticosteroid hormones CS and DCS are interpreted on the basis of DFT calculations. It was shown that the low-frequency lines in the Raman spectra belong to the skeletal vibrations of the molecules and the bending vibrations of the substituent at the C^{17} atom. On the whole, the calculated frequencies are in a good agreement with the experimental results. The discrepancies discussed in the paper are associated with the intermolecular interactions and the influence of crystal packing. In particular, the calculations predict the presence of 18 weak intermolecular interactions of the types of O···H and H···H in the tetramer of CS and 22 interactions in the tetramer of DCS with the total energy −36.9 and −49.1 kJ/mol, respectively, which stabilize the crystal cells. In the CS molecule, the strong intramolecular hydrogen bond $O^{21}-H\cdots O=C^{20}$ with the energy −42.4 kJ/mol and the intramolecular bond $O^{11}-H\cdots H(C^{19}H_3)$ with the energy −28.0 kJ/mol were revealed, which significantly govern the formation of the CS conformation.

In the optimization of the DCS dimer and the calculation of its Raman spectra by the DFT method in the B3LYP/6-31G(d) approximation, new intense low-frequency lines were obtained, which are caused by the intermolecular interaction and the mixing of normal vibrations of neighboring molecules in a molecular crystal. The active modes corresponding to intramolecular vibrations exhibit shifts and splittings in the Raman spectrum, which are clearly seen at low temperatures.

The different temperature dynamics of lines in the Raman spectra of CS and DCS is due to distinctions between nonvalence, intermolecular and intramolecular, interactions.

REFERENCES

1. K. Holderna-Natkaniec, A. Szyczewski, I. Natkaniec, V. D. Khavryutchenko, and A. Pawlukojc, Appl. Phys. A **74**, 1274 (2002).
2. A. Szyczewski, K. Holderna-Natkaniec, and I. Natkaniec, J. Mol. Struct. **693**, 49 (2004).
3. F. Parak, E. N. Frolov, R. L. Mossbauer, and V. I. Goldanskij, J. Mol. Biol. **145**, 825 (1981).
4. F. Mallamace, S. H. Chen, M. Broccio, C. Corsaro, V. Crupi, D. Majolino, V. Venuti, P. Baglioni, E. Fratini, C. Vannucci, and H. E. Stanley, J. Chem. Phys. **127**, 045104 (2007).
5. W. Doster, A. Bachleitner, R. Dunau, M. Hiebl, and E. Lüscher, Biophys. J. **50**, 213 (1986).
6. N. V. Surovtsev, V. K. Malinovsky, and E. V. Boldyreva, J. Chem. Phys. **134** (4), 045102 (2011).
7. O. P. Cherkasova, V. A. Volodin, V. A. Minaeva, B. F. Minaev, and G. V. Baryshnikov, Vestnik NGU, Ser. Fiz. **5** (4), 176 (2010).
8. O. P. Cherkasova, B. F. Minaev, G. V. Baryshnikov, L. I. Tkachenko, V. A. Minaeva, I. N. Smirnova, D. A. Sapozhnikov, A. V. Kargovsky, and A. P. Shkurinov, in *Theses of Reports on the ICONO/LAT Conferences (International Conference on Coherent and Nonlinear Optics (ICONO 2013) and International Conference on Lasers, Applications, and Technologies (LAT 2013))* (Moscow, 2013), p. JS83.
9. I. N. Smirnova, D. A. Sapozhnikov, A. V. Kargovsky, V. A. Volodin, O. P. Cherkasova, R. Bocquet, and A. P. Shkurinov, Vib. Spectrosc. **62**, 238 (2012).
10. V. A. Minaeva, B. F. Minaev, G. V. Baryshnikov, O. P. Cherkasova, A. A. Volodin, A. A. Slipets, E. V. Myshenko, and S. S. Kapinus, Visnik Cherkas'kogo Universitetu, Ser. Khim. Nauki, B **195** (1), 25 (2011).
11. V. O. Minaeva, B. P. Minaev, G. V. Baryshnikov, O. M. Romeiko, S. S. Kapinus, and O. P. Cherkasova, Visnik Cherkas'kogo Universitetu, Ser. Khim. Nauki, **195** (1), 49 (2011).
12. G. V. Baryshnikov, L. I. Tkachenko, V. O. Minaeva, B. P. Minaev, and O. P. Cherkasova, Visnik Cherkas'kogo Universitetu, No. **14** (267), 124 (2013).
13. G. P. Vinson, J. Endocrinol. **211**, 3 (2011).
14. A. D. Becke, J. Chem. Phys. **98**, 5648 (1993).
15. A. D. Becke, Phys. Rev. A **38** (6), 3098 (1988).
16. M. J. Frisch, G. W. Trucks, H. B. Schlegel, G. E. Scuseria, M. A. Robb, J. R. Cheeseman, J. A. Montgomeri, Jr., T. Vreven, K. N. Kudin, J. C. Burant, J. M. Millam, S. S. Iyengar, J. Tomasi, V. Barone, B. Mennucci, M. Cossi, G. Scalmani, N. Rega, G. A. Petersson, H. Nakatsuji, M. Hada, M. Ehara, K. Toyota, R. Fukuda, J. Hasegawa, M. Ishida, T. Nakajima, Y. Honda, O. Kitao, H. Nakai, M. Klene, X. Li, J. E. Knox, H. P. Hratchian, J. B. Cross, C. Adamo, J. Jaramillo, R. Gomperts, R. E. Stratmann, O. Yazyev, A. J. Austin, R. Cammi, C. Pomelli, J. W. Ochterski, P. Y. Ayala, K. Morokuma, G. A. Voth, P. Salvador, J. J. Dannenberg, V. G. Zakrzewski, S. Dapprich, A. D. Daniels, M. C. Strain, O. Farkas, D. K. Malick, A. D. Rabuck, K. Raghavachari, J. B. Foresman, J. V. Ortiz, Q. Cui, A. G. Baboul, S. Clifford, J. Cioslowski, B. B. Stefanov, G. Liu, A. Liashenko, P. Piskorz, I. Komaromi, R. L. Martin, D. J. Fox, T. Keith, M. A. Al-Laham, C. Y. Peng, A. Nanayakkara, M. Challacombe, P. M. W. Gill, B. Johnson, W. Chen, M. W. Wong, C. Gonzalez, and J. A. Pople, Gaussian 03, revision C.02 (Gaussian, Inc., Wallingford, 2004).
17. V. A. Minaeva, B. F. Minaev, and D. N. Hovorun, Ukr. Biokhim. Zh. **80** (4), 82 (2008).

18. H. Campsteyn, L. Dupont, O. Dideberg, and N. Mandel, Acta Crystallogr., Sect. B: Struct. Crystallogr. Cryst. Chem. **29**, 1726 (1973).
19. K. Shikii, H. Seki, S. Sakamoto, Y. Sei, H. Utsumie, and K. Yamaguchi, Chem. Pharm. Bull. **53** (7), 792 (2005).
20. W. L. Duax and D. A. Norton, *Atlas of Steroid Structure* (Plenum, New York, 1975), Vol. 1.
21. O. Dideberg, H. Campsteyn, and L. Dupont, Acta Crystallogr., Sect. B: Struct. Crystallogr. Cryst. Chem. **29**, 103 (1973).
22. R. Dey, S. Roychowdhury, P. Roychowdhury, and L. Righi, J. Chem. Crystallogr. **29** (12), 1271 (1999).
23. C. Lee, W. Yang, and R. G. Parr, Phys. Rev. B **37** (2), 785 (1988).
24. R. F. W. Bader, *Atoms in Molecules. A Quantum Theory* (Clarendon Press, Oxford, 1990).
25. E. Espinosa, E. Molins, and C. Lecomte, Chem. Phys. Lett. **285** (3) (1998).
26. E. Espinosa, I. Alkorta, and I. Rozas, Chem. Phys. Lett. **336** (5), 457 (2001).
27. R. Dey and P. Roychowdhury, J. Biomol. Struct. Dyn. **20** (1), 21 (2002).
28. L. Fieser and M. Fieser, *Steroids* (Reinholt, London, 1959).
29. J. C. Brookes, M. D. Galigniana, A. H. Harker, A. M. Stoneham, and G. P. Vinson, J. Roy. Soc. Interface **9**, 43 (2012).